Anaesthesia 2019, 74, 1406–1415 doi:10.1111/anae.14726

Original Article

The design and evaluation of a novel low-cost portable ventilator

A. Darwood,[1] **J. McCanny,**[2] **R. Kwasnicki,**[3] **B. Martin**[4] and **P. Jones**[4]

1 PhD candidate and Foundation Doctor, 2 Registrar, Department of Anaesthesia, 3 Senior House Officer, Department of Plastic Surgery, Imperial College Healthcare NHS Trust, London, UK
4 Consultant, Department of Anaesthesia, St. Bartholomew's Hospital, London, UK

Summary

Modern mechanical ventilator technologies broadly consist of digitally-controlled electronic devices and analogue systems driven by compressed gas sources. Drawbacks such as high cost, complex maintenance and the need for cumbersome sources of compressed driving gas hinder adoption in pre-hospital and low-resource environments. We describe the evaluation and testing of a simple, low-cost alternative ventilator that uses a novel pressure-sensing approach and control algorithm. This is designed to provide portable positive-pressure mechanical ventilation at a reduced cost, while autonomously monitoring patient condition and important safety parameters. A prototype ventilator was constructed and evaluated using an anaesthetic test-lung as a patient surrogate. Using a modifiable test-lung and digital pressure sensor, we investigated ventilation pressure waveform circuit leak detection, and compliance and resistance change detection. During intermittent positive-pressure ventilation to the test-lung, the prototype system showed acceptable pressure waveform parameters: all simulated circuit leaks ≥ 6 mm^2 in size were detected; compliance changes were detected between 10 ml.cmH_2O^{-1}, 20 ml.cmH_2O^{-1} and 50 ml.cmH_2O^{-1}; and resistance changes were detected across the available simulated range. These results show this prototype technology has the potential to provide safe emergency ventilation without the use of any complex digital sensors or software while its construction and design enables significant reductions in cost and complexity. The study suggests further work is now justified in progressing the technology to clinical trials.

Correspondence to: A. Darwood
Email: alastairdarwood@hotmail.com
Accepted: 8 May 2019
Keywords: invasive ventilation; mechanical ventilator; pre-hospital medicine; transfer medicine; transport ventilator
This article is accompanied by an editorial by Young, *Anaesthesia* 2019; **74**: 1357–60 and an article by Williams et al., *Anaesthesia* 2019; **74**: 1416–24.

Introduction

Mechanical ventilation is an essential component in the delivery of modern critical care, peri-operative practice and transfer medicine. Ventilators are mandatory in hospital-based environments and are ubiquitous in pre-hospital settings [1, 2]. Although safe and reliable, modern devices remain hampered by high costs, reliance on inconvenient consumables such as compressed gas supplies, and practical inefficiencies such as size and complexity. These issues are particularly pertinent in relation to transport or emergency ventilators for which convenience, size and cost are paramount.

Modern microprocessor-controlled electronic devices have high manufacturing and maintenance costs, while pneumatic-powered alternatives lack durability and resilience by virtue of the complexity of their component parts and reliance on a source of compressed gas [3]. Hand-delivered positive-pressure ventilation systems such as bag-valve masks

are commonly used for short-term ventilation but prevent the operator from simultaneously performing other crucial clinical interventions [3]. As imprecise techniques, they also potentially expose the patient to greater risk from volutrauma, barotrauma and hyperventilation [3].

Complex, high-tolerance digital pressure sensors and pneumatic components, in addition to multilayered software, contribute to the high cost and mechanical or electrical liability of many technologies [4]. Such bulky and delicate equipment is not ideal when working in extreme, remote or austere environments with limited space, personnel and resources. In addition, the high economic cost and complexity of existing technologies creates difficulties in the deployment of sufficient ventilators in the event of a mass casualty situation. Current approaches mandate the triaging of ventilator usage [5]; however, a low-cost alternative technology may provide a scalable solution to this issue. A new approach is required that is capable of providing safe, reliable portable ventilation to those patients who need it most [6].

We describe the development and evaluation of a simple and inexpensive electromechanical ventilator that uniquely functions by the use of an adjustable single pole, single-throw pressure-sensitive switch as its sole controlling sensor. Our novel ventilator also has the potential to integrate patient safety monitoring capabilities.

Methods

A prototype ventilator was constructed with readily available electrical components including an electric motor connected to a centrifugal impeller (Micronel UK Ltd, Winsdor, UK) to provide airflow. The ventilator consists of two separate hardware elements: a single-use 'disposable' patient connection element; and a re-usable powered 'motor unit'. A ventilator schematic is shown in Fig. 1.

The disposable unit consists of a repurposed exhaust valve assembly from a conventional bag-valve mask with an

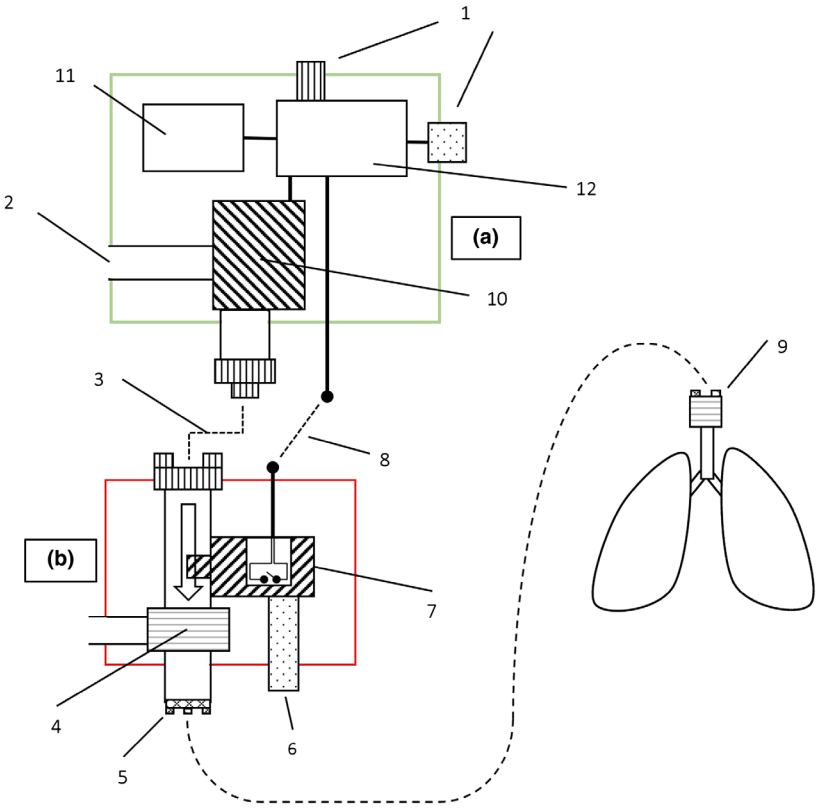

Figure 1 Ventilator design schematic showing all component parts of the motor unit (a) and disposable unit (b). 1. control dials and buttons; 2. air intake; 3. airflow coupling between motor and disposable unit; 4. exhaust valve; 5. coupling to lungs (i.e. tracheal tube connection); 6. switch threshold selection dial; 7. pressure-sensitive mechanical (ON/OFF) switch; 8. electrical connection between disposable and motor unit; 9. tracheal tube (or other airway interface) and patient's lungs; 10. motor and impeller with electronic speed controller (ESC); 11. power source (e.g. batteries); and 12. microcontroller.

added pressure-sensitive switch. Standardised 22-mm (male) and 15-mm (female) connectors facilitate ventilator connection to a patient airway interface, for example, a tracheal tube. The pressure-sensitive mechanical switch operates at a user-defined threshold which may be set at 10–45 cmH_2O by means of a dial. This assembly is reversibly attached to the re-usable motor unit comprising a motor, controller and power source. Atmospheric air is entrained by the motor unit and delivered through the disposable unit to the patient end. Expired gas is released to the atmosphere by means of the exhaust valve, located in the disposable unit, thus protecting the motor unit from contamination. The pressure-sensitive switch on the disposable unit is electrically coupled to the 'motor unit'. Algorithms describing the proposed ventilator function were encoded and written to a simple commercially available microcontroller (Arduino® Nano PCB with ATmega328 chip; Arduino organisation, Ivrea, Italy) which is integrated into the prototype and connected to the impeller motor via a commercially available electronic speed controller (ESC). The ESC is configured to enable variable motor throttle (torque control) between 0% and 100% including electronic braking from any speed; this allows the motor to be stopped rapidly when required. Function buttons and selection dials allow the operator to set a respiratory rate and inspiratory to expiratory (I:E) ratio. Desired peak pressure is selected using the threshold adjustment dial for the pressure-sensitive switch. The unpackaged test prototype is shown in Fig. 2.

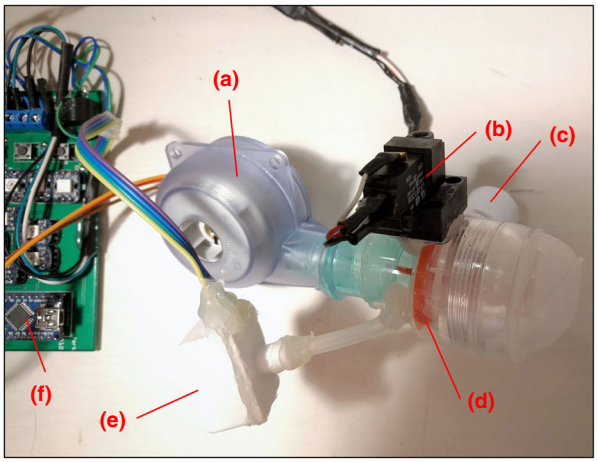

Figure 2 Unpacked test rig prototype: (a) motor and impeller; (b) pressure-sensitive mechanical switch; (c) patient connection; (d) exhaust valve; (e) external pressure sensor (for experimental purposes); and (f) control board and microcontroller.

Like a domestic light switch, the pressure-sensitive switch within the disposable component is only able to be ON or OFF depending on the applied pressure being above or below the user-specified threshold. As the switch is within the disposable component, the pressure at the switch corresponds with patient airway pressure. As no other sensors are present in the device, the status of the mechanical switch (ON or OFF) is the only patient feedback provided to the device microcontroller in the re-usable component. As a result, control algorithms must provide full ventilation solely using the mechanical switch status. A detailed description of algorithm design and function is available in the appendix.

When the ventilator is first initialised and connected to a patient, a calibration protocol is automatically carried out that allows the device to identify what motor throttle is required to achieve the required peak pressure (Fig. 3). The device has no way of identifying the actual ventilation pressure it is providing; rather, the switch status (ON or OFF) indicates when the threshold pressure, and thus ventilation pressure, has been reached by means of changing its configuration or 'tripping'. The corresponding motor throttle value is saved and used for further ventilator operation. Once calibration is complete, the device enters a 'ventilation mode' in which continuous breaths are

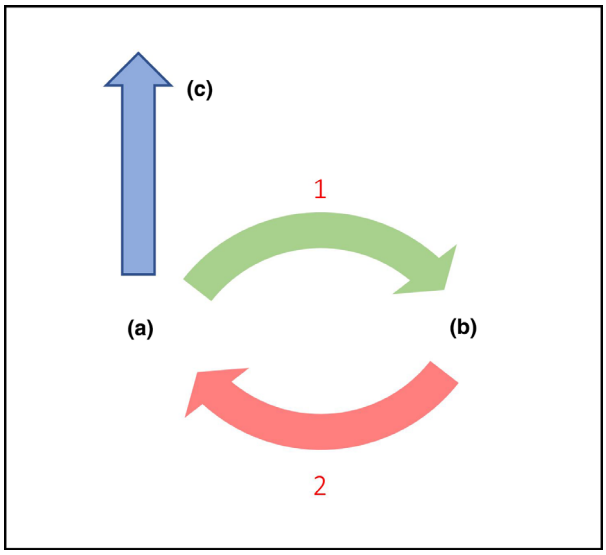

Figure 3 Ventilator control algorithm overview. Calibration mode (a) allows mapping of patient airway and circuit conditions to optimise ventilator function. Successful calibration (1) allows algorithm to progress to normal ventilation mode (b). If a safety alert is detected, for example, leak, or a large change in resistance or compliance (2) the algorithm returns to calibration mode (a). If there are serial failed calibration attempts then a major alarm is sounded (c).

delivered at the calibration-derived throttle value until one of two events occurs: the battery pack is exhausted; a or a safety alert is triggered (Fig. 3). With feedback from the pressure-sensitive switch, the device is able to detect hardware failure, circuit leak, and changes in resistance or compliance (as evaluated in this experiment), providing appropriate alarms as required. In addition, given small variations in these parameters, calibration mode is automatically re-entered allowing attempts at compensation and continued ventilation. Should recalibration fail, for example, due to an extremely large leak or hardware failure in the disposable unit, an appropriate alarm is used to alert the user. In any given 'breath', the time taken from the moment the motor starts, to the moment the threshold pressure is achieved (thus tripping the switch), is measured and is recorded as the variable 'time to reach pressure' (TRP) measured in milliseconds (ms). It was recognised that this TRP metric may vary with changing lung conditions and experiments were conducted to study how the prototype behaved.

A prototype was configured and connected to an anaesthetic test-lung (Fig. 4) capable of simulating different compliance levels, airway resistance levels and degree of circuit leak. As the ventilator has no digital pressure sensor, an external sensor (Bosch® BMP180; Bosch Sensortec GmbH, Reutlingen, Germany) was temporarily connected to the disposable component during the experiment so that live pressure data could be fed back to a data-capture laptop computer. The sensor was factory calibrated and accurate to ± 0.3 cmH_2O enabling ventilator performance to be assessed. The prototype was configured to sequentially record the TRP values of each breath. The prototype was additionally modified such that the TRP value was also sent to the data-capture laptop. Accordingly, both the delivered pressure and the TRP values, could be recorded in real-time for subsequent analysis.

Performance during changes in compliance was assessed first. The pressure-sensitive switch was set to a given threshold level and the ventilator was initiated at a rate of 10 breaths.min^{-1} with an inspired:expired (I:E) ratio of 1:1. The test-lung was configured to its maximally compliant state. Ten breaths were carried out while sequentially recording the TRP values of each breath. After the 10th breath, the test-lung compliance was reduced from 100 to 50 ml.cmH_2O^{-1}. After a one-breath period of equilibrium, the subsequent 10 breaths were recorded as above. Finally, test-lung compliance was again reduced to 10 ml.cmH_2O^{-1} for a further 10 breaths. The entire procedure was performed at each of three peak pressure levels: 16 cmH_2O; 20.8 cmH_2O; and 34.2 cmH_2O.

Performance during changes in airway resistance was assessed in a similar manner, except that resistance in the ventilator tubing, as opposed to compliance, was sequentially changed every 10 breaths at each of the peak pressures chosen. In these tests, the compliance of the test-lung was kept constant and set at a nominal physiological level. Resistance levels assessed were: baseline (no additional resistance); 5 cmH_2O. $l^{-1}.s^{-1}$; 20 cmH_2O. $l^{-1}.s^{-1}$; 50 $cmH_2O.l^{-1}.s^{-1}$; and 200 cmH_2O. $l^{-1}.s^{-1}$.

Performance during varying degrees of circuit leak was assessed making use of the test-lung's 'leak' feature. A threaded screw was gradually removed, creating an increasing circuit leak with a maximum leak hole area of 20 mm^2. The effect of increasing leak was assessed over each of the chosen inspiratory pressures. Change in TRP was recorded, in addition to whether the system returned to calibration mode within two breaths as a result of the leak.

Results

Figure 5 shows a screenshot from the data-capture computer displaying a sample pressure vs. time graph (ventilation pressure 28 cmH_2O, rate 10 breaths.min^{-1}, I:E ratio 1:1). The increasing form exponential decay pressure–time relationship from the point the motor starts to the peak pressure corresponding to achieving the switch trip threshold is demonstrated.

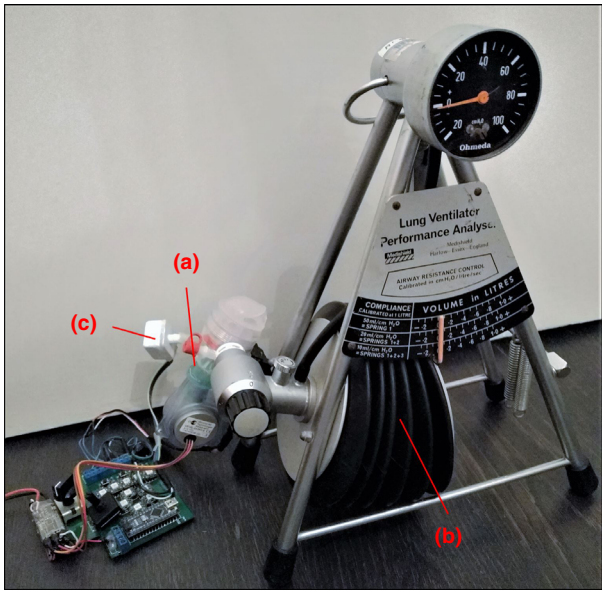

Figure 4 Unpacked 'test rig' prototype (a) connected to adult anaesthetic test-lung (b) during experiment. Experimental digital pressure sensor (c) connected to data-capture computer (not shown).

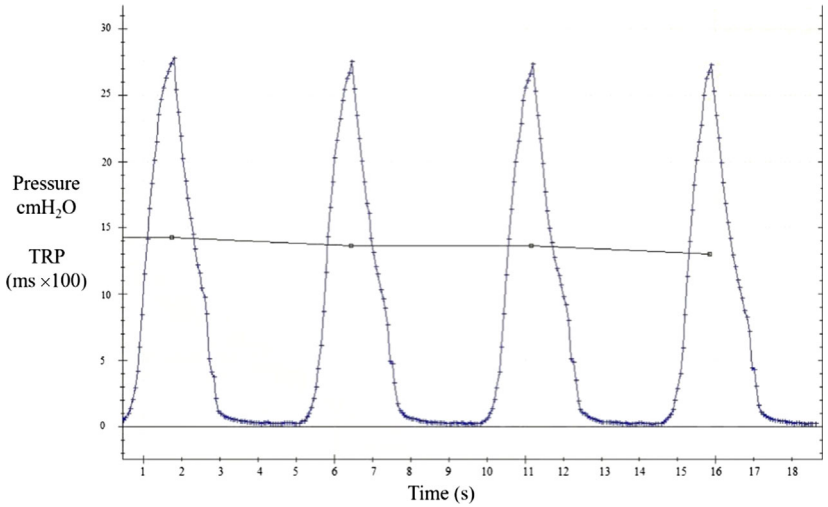

Figure 5 Computer screenshot captured from the data-capture software during the experiment. The y-axis shows both the time to reach pressure/100 (○) and pressure (cmH_2O) (—). The screenshot shows the increasing form exponential decay curve achieved during ventilation at 28 cmH_2O at a physiological respiratory rate. TRP, time to reach pressure.

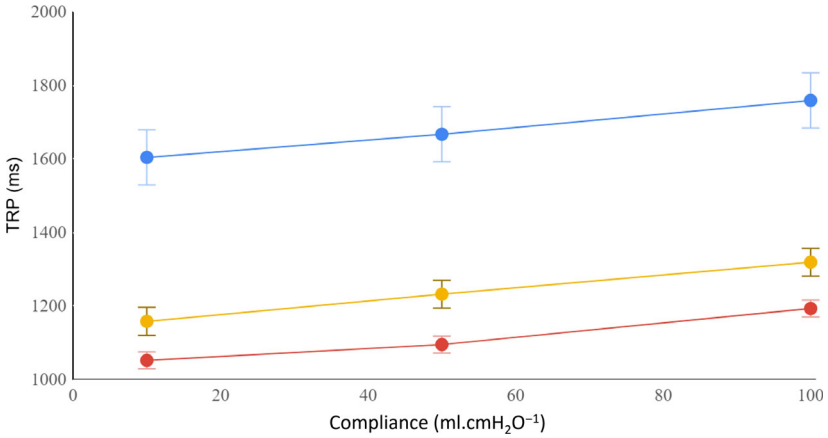

Figure 6 Time to reach pressure (TRP) value with changes in compliance at different physiological ventilation pressures (yellow = 16 cmH_2O; red = 20.8 cmH_2O; and blue = 34.2 cmH_2O). Error bars indicate standard deviation across each pressure group.

The experiments showed how the TRP value of each breath varies with changing test-lung characteristics. In other words, how the time taken between the motor starting and the pressure-sensitive switch 'tripping' on each delivered breath varies when circuit parameters are changed.

As test-lung compliance was increased, the measured TRP value increased, a trend observed across each pressure group (Fig. 6). For example, in the highest ventilation pressure group, the measured mean (SD) TRP value was 1605 (74) ms at a test-lung compliance of 10 $ml.cmH_2O^{-1}$. This means it took on average 1605 ms for the pressure to reach the threshold pressure on the pressure-sensitive switch.

Figure 7 shows the effect on TRP value with increasing flow resistance in the test-lung circuit. Initially there was an increase in TRP value with rising resistance values until a maximum of 20 $cmH_2O.l^{-1}.s^{-1}$ was reached. Then, at higher resistance values, the TRP decreased as airway resistance was further increased and restricted flow to the point that peak pressure was achieved due to the airway obstruction itself.

Figure 8 shows the TRP with varying circuit leaks in the test-lung device. A small circuit leak (6 mm^2 diameter hole)

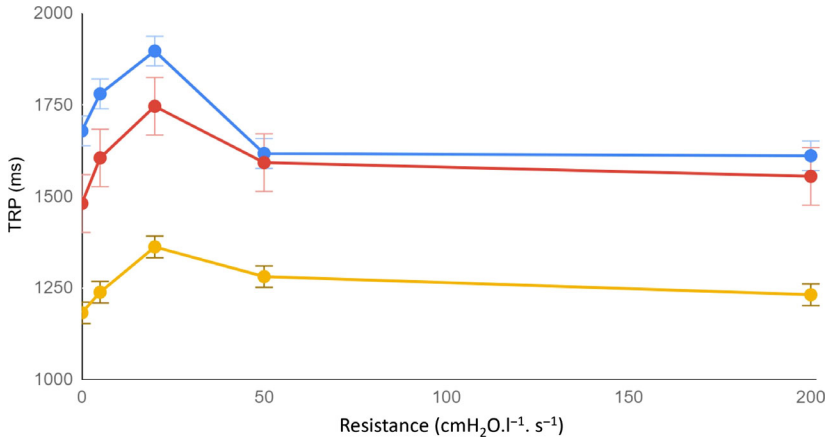

Figure 7 Time to reach pressure (TRP) value with changes in airway resistance at different physiological ventilation pressures (yellow = 16 cmH_2O; red = 20.8 cmH_2O; and blue = 34.2 cmH_2O). Error bars indicate standard deviation across each pressure group.

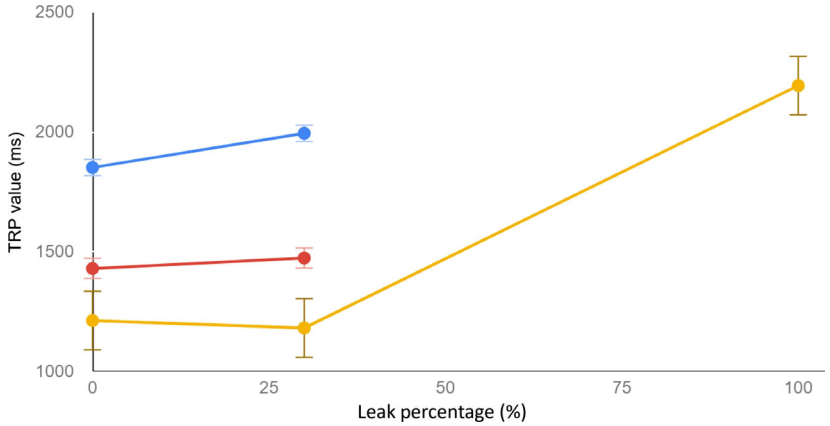

Figure 8 Time to reach pressure (TRP) value with different air leakages at different physiological ventilation pressures (yellow = 16 cmH_2O; red = 20.8 cmH_2O; and blue = 34.2 cmH_2O). Error bars indicate standard deviation across each pressure group.

allowed ventilation to proceed albeit with increased TRP values. When the circuit leak was increased to a maximum hole area of 20 mm^2 this resulted in a failed breath and a return to calibration mode in order to re-adapt to the new airway circuit conditions. This is reflected in the results by the lack of data-points for the two higher pressure groups.

Discussion

Our experimental data indicate that our novel device may successfully provide the most important functions of a mechanical ventilator, namely: accuracy; reliability; and safety in the delivery of user-specified ventilator settings. Crucially, the use of a pressure-sensitive binary switch allows the design and construction to remain low-cost providing a compact, easily transportable ventilator solution with a single moving part.

Unlike conventional ventilators where real-time patient pressure and flow data are often available, our ventilator is limited to one single binary datum point during each breath indicating whether the pressure is above or below the user-specified threshold. Of note, the ventilator controller remains 'unaware' of the absolute pressure during the respiratory cycle – the peak pressure is entirely user determined during setup with the adjustment dial on the pressure-sensitive switch. As the binary pressure-sensitive switch provides the only monitoring information, the controlling algorithms remain simple; this in contrast to the complex software layers present on some current digital approaches.

To maximise clinical relevance, we tested whether the proposed ventilator was capable of detecting and indicating the most important clinical and performance metrics,

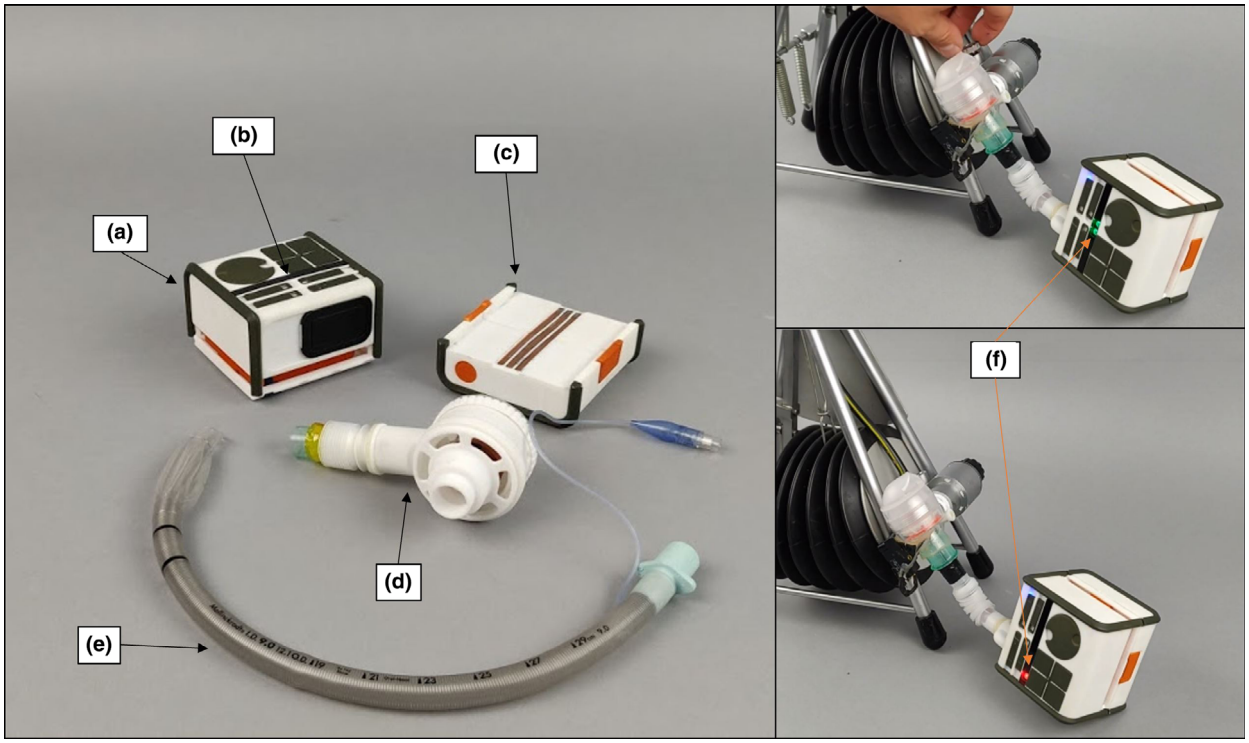

Figure 9 Fully functional prototype ventilator showing constituent parts: (a) motor unit; (b) light-emitting diode (LED) indicators; (c) battery pack, (d) disposable unit; and (e) armoured tracheal tube (internal diameter 9.0 mm). B: Prototype ventilator demonstrating LED light shift (f) as leak is introduced in the circuit.

namely changes in compliance, resistance and circuit leakages. We investigated the relationship between the measured TRP value and changing test-lung circuit parameters, potentially allowing this metric to infer changes in a ventilated patient's clinical condition without the need for any complex digital sensors or software. Although the absence of digital sensors prevents the calculation of absolute numerical values for tidal volume (and hence compliance), our approach can provide an indication of change for further investigation by the user. As such, ventilation modes are entirely of a pressure-controlled variety. For example, Fig. 9 shows a proof of concept of a pre-clinical prototype device that was constructed in the above manner. In this case, a line of 10 indicator lights was provided indicating any change in the TRP value. Following calibration, a green light illuminates in the middle of the light strip. Any subsequent change in the TRP value is depicted by illuminating a light further along the strip. In the case of Fig. 9, a leak is introduced in the system with a corresponding change in the illuminated LED position and colour. For every 30-ms difference in TRP value, the next indicator light was illuminated (with an optional alarm tone of increasing severity). In this way, an attending clinician may be rapidly alerted to both the magnitude and direction of any change in the TRP value and thus deduce the relevant clinical issue.

Changes in resistance and compliance may indicate mucus plugging, bronchospasm, massive haemothorax, tension pneumothorax or acute lung injury. It is important to alert users to such changes. The pressure-sensitive switch reaches threshold and 'trips' as soon as gas flow and pressure are at equilibrium (where gas flow is at a minimum and pressure is at a maximum) and our results showed that decreased compliance resulted in a decreased TRP value. When compliance decreases, stiffer lungs cause a faster pressure rise, so equilibrium between the motor unit and the lungs is reached faster, resulting in a decreased TRP value. With increased compliance, the converse is true and a longer time is needed to reach equilibrium as a larger volume of gas is delivered to the lungs. As airway resistance increases, gas flow reduces, hence a longer time is needed to reach equilibrium with a correspondingly larger TRP value. When resistance is extremely high, conducting airways are so narrow they act as an effective obstruction, thus forcing equilibrium to occur prematurely, and producing a fall in TRP.

Circuit leak was readily identified, even for small leaks in the patient circuit. It is important to remember that the ventilator's calibration protocol allows identification of the specific throttle value required to generate a sufficient peak pressure to trip the switch. Control algorithms apply a small multiplicative factor to this value to create an 'overshoot'. This overshoot ensures that natural, minor fluctuations in motor function do not prevent the required pressure threshold being achieved on each delivered breath. This overshoot (3.0–4.5%) manifests as the observation that very small leaks are tolerated, with an increase in TRP being seen, as expected. If the leak is made bigger, the specific calibration-derived throttle value is insufficient to achieve the desired threshold pressure, and hence the breath 'fails'. As seen experimentally, this merely causes a return to calibration mode, thus alerting the user to a change in the breathing system's status as well as adaptation to the circuit leak up to a point.

In summary, the results show a reliable variation in the average TRP value as physiologically relevant circuit characteristics are varied. This effect may be useful in detecting potential pathophysiological change in a patient when using this novel ventilator in the absence of conventional pressure and flow sensors.

The current benchtop study device and pre-clinical protype (Fig. 9) are capable of full pressure-controlled ventilation at a user-specified rate (5–30 breaths.min^{-1}), peak pressure (10–45 cmH_2O) and user-specified I:E ratio. The device is powered by four commercially available 18650 lithium ion cells providing around 6 h of battery life. The design facilitates 'hot-swapping' of battery packs and reverse polarity insertion protection while keeping size and weight extremely low – the functional device weighs approximately 450 g and is able to fit comfortably into most equipment pockets. The existing design allows the optional use of supplementary oxygen which may be delivered through a low-pressure port in the side of the device and flow titrated to provide a desired gas mix. Positive end-expiratory pressure may be provided with a conventional exhaust restricting valve fitted to the disposable unit. Leak detection facility along with the ability to deliver high flow rates allow the use of non-secure airway interfaces such as supraglottic airway devices or facemasks.

At present, the prototype device requires an intravenous infusion anaesthetic technique. However, it is envisaged that accessories may be designed allowing integration with conventional draw-over inhaled anaesthetic delivery systems. Such systems may be positioned at the air intake allowing vapour to be drawn through the ventilator and delivered to the patient. As patient feedback is limited to the binary pressure-sensitive switch output, conventional waveform monitoring or the provision of exact numerical values for tidal volume, lung compliance or circuit leak is not possible without added accessories. Clinicians are, instead, provided with a sensitive indicator of changing conditions as discussed above. In addition, dynamic motor throttle control above the calibration-derived throttle value would be unsafe, hence very high respiratory rates are not available (> 30 breaths.min^{-1}).

As the TRP value is extremely sensitive to lung (and thus circuit) conditions, any significant modification to either of the above may result in inaccurate readings when using the existing prototype. For example, if connecting tubing lengths > 50 cm are used, the TRP metric would require calibration to remain accurate due to the increased non-compliant dead space volume. Similarly, if the current prototype were to be connected to a paediatric patient with small lungs (< 30 kg), the TRP value would again require calibration as the small volumes would result in comparatively rapid filling with smaller variation as compliance changed. In practice, these limitations may be addressed with simple fixed calibration settings that a user may select such as a switch or slider for selecting between paediatric or adult patients. To date, the device has only been assessed on adult test-lung equipment with standardised tubing lengths. Tubing has been specifically designed to make use of the extremely small ventilator footprint allowing the ventilator to remain as close as possible to the airway. At this early stage, it is challenging to provide accurate final production costs; however, the authors envisage these to be significantly lower than comparable devices due to device simplicity and the lack of any complex parts or digital control components. The authors hope and expect final device manufacturing costs will be below £150 (€174, US$ 195) per unit with disposable costs at a similar price to existing disposable bag-valve mask products currently on the market. Mass manufacture and scaled production may help to lower these costs in the future.

With simple algorithm changes and slight hardware modifications, further ventilation modes are possible. For example, a redesigned 'disposable unit' incorporating a switch with both a positive and negative pressure threshold could allow the device to respond to patient-generated negative pressures. This would allow modes to include triggering of synchronised, assisted positive-pressure support during spontaneous ventilation. Further development work is directed towards device validation in an in-vivo setting with eventual application for a CE mark and United States Federal Drug Administration approval.

In conclusion, this proof of concept study provides evidence that a single adjustable pressure-sensitive switch can safely and effectively deliver mandatory mechanical ventilation. We have demonstrated that this simple, yet novel, approach can drive mechanical ventilators that are compact, portable, robust and reliable. Furthermore, the pragmatic design enables low production cost, minimal component maintenance and greater resilience while reliably performing key ventilator functions. Its simplicity, mechanical resilience and economic cost-effectiveness represents an affordable ventilator solution for the most challenging and low-resource environments that clinicians encounter. It is hoped that this novel technology may provide access to simple, safe ventilation in healthcare settings that are unable to afford full-function digital devices and would struggle with the necessary infrastructure to provide a supply of compressed gas to power conventional pneumatic devices.

For all these reasons, the authors envisage that further development of this novel technology will offer considerable advantages over conventional ventilators for clinicians in specific settings. Further in-vivo work with clinicians is planned to optimise functional adaptations and provide reliable ventilator solutions in low-resource settings, wilderness and expedition medicine, as well as during pre-, inter- and intrahospital transport of critical care patients.

Acknowledgements

The authors thank product design advisor A. Dawood who designed and prototyped the product embodiment shown in Fig. 9. In addition, Colonel P. Mahoney and Colonel D. Parkhouse provided invaluable expertise and support to the project in reaching its current stage of development. At the time of writing, corresponding author A. Darwood is the owner of UK patent application GB2018/052029 detailing the above invention. No external funding or other competing interests declared.

References

1. Schmid M, Mang H, Ey K, Schüttler J. Prehospital airway management on rescue helicopters in the United Kingdom. *Anaesthesia* 2009; **64**: 625–31.
2. Lockey DJ, Crewdson K, Davies G, et al. AAGBI: safer pre-hospital anaesthesia 2017. *Anaesthesia* 2017; **72**: 379–90.
3. Holets SR, Davies JD. Should a portable ventilator be used in all in-hospital transports? *Respiratory Care* 2016; **61**: 839–53.
4. Beckmann U, Gillies D, Berenholtz S, Wu A, Pronovost P. Incidents relating to the intra-hospital transfer of critically ill patients. *Intensive Care Medicine* 2004; **30**: 1579–85.
5. Powell T, Christ KC, Birkhead GS. Allocation of ventilators in a public health disaster. *Disaster Medisine Public Health Preparedness* 2008; **2**: 20–6.
6. Krishnamoorthy V, Vavilala MS, Mock CN. The need for ventilators in the developing world: an opportunity to improve care and save lives. *Journal of Global Health* 2004; **4**: 010303.

Appendix. Detailed description of the ventilator control algorithm function

The pressure-sensitive switch is directly connected to the microcontroller by means of the electrical connection between the disposable unit and the re-usable unit. The switch may be 'open', thus preventing electrical current from flowing, or 'closed', allowing electrical current to flow. If pressure at the switch is above threshold pressure, the switch is 'closed' allowing current to flow. If pressure at the switch is below threshold pressure, the switch is 'open', preventing electrical current flow. In this way, two binary options are presented to the microcontroller. The switch is positioned such that it may measure airway pressure thus the binary switch state is representative of airway pressure with respect to a user-defined threshold. Algorithms were designed to provide successful ventilation and monitoring information relying exclusively on these solitary, binary signal options, with no other sensor input. An overall algorithm schematic is shown in Fig. 3 beginning with an initial calibration phase.

Once connected to the subject, a calibration step is performed allowing the device to configure algorithm variables to the current patient and circuit conditions. The system must 'learn' the correct maximum motor throttle value to achieve the chosen peak pressure, and this is determined by the minimum throttle required to reach switch pressure threshold. This is achieved with a slow (4 s) linear throttle rise towards maximum, from stationary, until the threshold peak pressure is reached, causing the switch to trip. The throttle value at this point is recorded to controller memory.

The ventilator now enters 'ventilation mode'. This continuously delivers breaths to a patient at a rate chosen by the user, for the duration of available battery life unless an error is detected, which prompts a return to the calibration protocol. To provide a breath in 'ventilation mode', the motor is immediately started at the calibration-derived throttle value. As the motor accelerates, pressure increases as air flows into the test-lung (following an increasing form exponential decay curve). Pressure continues to rise as the lung distends until threshold pressure is reached causing the pressure-sensitive switch to trip. This change in switch status alerts the controller that the pre-set pressure has been successfully achieved.

As soon as the switch trips, the motor throttle is rapidly reduced, which results in a reduction in circuit pressure

and resetting of the switch. The motor subsequently continues at this throttle value until inspiratory time elapses. The motor is then stopped (or reduced to a minor speed) for the duration of available exhalation time to allow the lungs to passively empty to the atmosphere via the 'disposable unit' exhaust valve.

Safety considerations

1 Circuit leak. If a new leak develops, the throttle value derived during the calibration protocol may no longer be sufficient to trip the pressure sensitive switch. In this case, a "full inspiration time" will elapse without tripping the pressure switch. This prompts the ventilator to re-enter the calibration protocol such that it may readjust to the new circuit conditions, and compensate for the leak.
2 Hardware failure. The pressure-sensitive switch may malfunction in one of two ways. In both cases, the operator is informed of the error and must replace the faulty component.

    a Failure to 'trip' despite threshold pressure being reached. This scenario is detected with a safety stop in the 'calibration' phase. This safety stop is placed at a throttle value where the maximum possible static pressure is known and is above usual ventilation pressures (e.g. 30 cmH_2O). The desired ventilation pressure set by the user will likely be lower than this. Thus, if the safety stop value is met during calibration, hardware failure is suggested if there is no leak. If ventilation is indeed required at pressures in excess of the safety value, the operator may allow calibration to proceed past the safety value using an override button.
    b Failure of switch to reset despite pressure dropping below threshold pressure. This failure mode is automatically detected as the switch must necessarily reset whenever the motor throttle significantly drops such as during exhalation. If the switch remains in its 'above threshold' status despite the motor being at very low throttle values, a clear hardware error has occurred and the switch requires replacement.

Compliance and resistance detection

In any given 'breath', the time taken from the moment the motor starts, to the moment the threshold pressure is achieved (thus tripping the switch), is measured and is recorded as the variable 'Time to Reach Pressure' (TRP) measured in milliseconds (ms). It was recognised this TRP metric may vary with changing lung conditions and experiments were conducted to study how the prototype behaved.